Six- vs Seven-Membered Ring Formation from the 1-Bicyclo[4.1.0]heptanylmethyl Radical: Synthetic and ab Initio Studies†

Eric J. Kantorowski, Shawn W. E. Eisenberg,‡ William H. Fink,* and Mark J. Kurth*

Department of Chemistry, University of California, Davis, California 95616

Received August 21, 1998

The viability of utilizing 1-bicyclo[4.1.0]heptanylmethyl radical (**3**) to serve as a progenitor of seven-membered carbocycles was examined. Rate constants for the rearrangement of this radical to 3-methylenecycloheptyl radical (**4**) and 2-methylenecyclohexyl-1-methyl radical (**6**) were measured using the competition method of **3** with thiophenol over the temperature range of −75 to 59 °C. Arrhenius functions were calculated for the conversions of **3** to **4** and **3** to **6** and found to be $\log(k/s^{-1}) = (12.38 \pm 0.20) - (5.63 \pm 0.23)/\theta$ and $\log(k/s^{-1}) = (11.54 \pm 0.32) - (5.26 \pm 0.37)/\theta$, respectively. The rate constants for these conversions at 25 °C are 1.86×10^8 s^{-1} and 5.11×10^7 s^{-1}, respectively. Hence, the seven-membered ring-expanded carbocycle is formed 3.6 times faster at 25 °C than the nonexpanded species. This suggests that the 1-bicyclo[4.1.0]heptanylmethyl radical system may be synthetically useful in seven-membered ring-forming methodology. Preliminary theoretical examination of this radical system qualitatively predicted the experimentally determined energies of activation: PMP4/6-31G*//HF/6-31G* ΔE_a (**3** → **6** − **3** → **4**) = 3.0 kcal/mol with zero point energy correction. The HF/6-31G* optimized reaction coordinate stationary points suggest cyclopropyl substituent eclipsing interactions play an important role in determining the kinetic outcome of these rearrangements.

Introduction

Rearrangement of cyclopropylcarbinyl radical systems to the corresponding 3-butenyl radicals has received much attention both in synthetic and theoretical settings.[1] The kinetics of the prototypical system have been thoroughly studied by many research groups employing techniques such as ESR, NMR, and product analysis.[2] Once kinetic data is established[3] for a distinct radical rearrangement, it may be applied as a radical "clock" against other radical reactions thereby providing a tool for mechanistic investigation.[4] Making substitutions to the parent system significantly affects the rate of bond rupture, and consequently a diverse range of radical clocks may be developed.[5] Additionally, there is great interest in the application of molecular modeling analysis to assist in predicting energies associated with the modified archetypal system.[6] As information on these systems increases, their viability as synthetic tools also advances.[7]

We were interested in employing radical **3** as part of a larger methodology for the preparation of seven-membered rings (Scheme 1). In this strategy, radical precursor **2** would be accessed via cyclopropanation of Diels−Alder-derived cyclohexene **1**. This cycloaddition reaction, which can set up to four contiguous stereocenters, could then be elaborated to **5** by the route shown. When the cyclopropane ring is substituted, this methodology would allow for introduction of a fifth stereocenter where neighboring stereocenters could influence the facial approach of the reducing agent to the singly occupied molecular orbital (SOMO). In addition to the ease of preparing cyclohexenyl systems, carbon-centered radicals are tolerant of hydroxyl and amine functionalities, thereby allowing a synthetic plan to forego the use of protecting groups which might otherwise be required for an ionic ring-forming process.

Central to the application of radicals in a synthetic setting is the need to have well-established rate data for all of the significant reaction pathways involved. The ability to predict the outcome is critical for any synthetic endeavor whose success depends on a tandem radical process.[8,9] Beyond this first criterion, there is a funda-

† Dedicated to Professor R. Bryan Miller, deceased October 29, 1998.

‡ Current address: AMGEN, One Amgen Center Drive, Thousand Oaks, CA 91320-1789.

(1) (a) Montgomery, L. K.; Matt, J. W.; Webster, J. R. *J. Am. Chem. Soc.* **1967**, *89*, 923−934. (b) Montgomery, L. K.; Matt, J. W. *J. Am. Chem. Soc.* **1967**, *89*, 934−941. (c) Mariano, P. S.; Bay, E. *J. Org. Chem.* **1980**, *45*, 1763−1769. (d) Kochi, J. K.; Krusic, P. J.; Eaton, D. R. *J. Am. Chem. Soc.* **1969**, *91*, 1877−1879.

(2) (a) Newcomb, M.; Glenn, A. G.; Williams, W. G. *J. Org. Chem.* **1989**, *54*, 2675−2681. (b) Beckwith, A. L. J.; Bowry, V. W. *J. Org. Chem.* **1989**, *54*, 2681−2688. (c) Newcomb, M.; Tanaka, N.; Bouvier, A.; Tronche, C.; Horner, J. H.; Musa, O. M.; Martinez, F. N. *J. Am. Chem. Soc.* **1996**, *118*, 8505−8506.

(3) For an excellent introduction to kinetic analysis of such systems see: Newcomb, M. *Tetrahedron* **1993**, *49*, 1151−1176.

(4) (a) Griller, D.; Ingold, K. U. *Acc. Chem. Res.* **1980**, *13*, 317−323. (b) Engel, P. S.; Wu, A. *J. Org. Chem.* **1994**, *59*, 3969−3974. (c) Beckwith, A. L. J.; Bowry, V. W. *J. Am. Chem. Soc.* **1994**, *116*, 2710−2716. (d) Caldwell, R. A.; Zhou, L. *J. Am. Chem. Soc.* **1994**, *116*, 2271−2275.

(5) (a) Tadic-Biadatti, M.-H. L.; Newcomb, M. *J. Chem. Soc., Perkin Trans. 2* **1996**, 1467−1473. (b) Choi, S.-Y.; Newcomb, M. *Tetrahedron* **1995**, *51*, 657−664. (c) Martin-Esker, A. A.; Johnson, C. C.; Horner, J. H.; Newcomb, M. *J. Am. Chem. Soc.* **1994**, *116*, 9174−9181. (d) Newcomb, M.; Choi, S.-Y. *Tetrahedron Lett.* **1993**, *34*, 6363−6364.

(6) (a) Martinez, F. N.; Schlegel, H. B.; Newcomb, M. *J. Org. Chem.* **1998**, *63*, 3618−3623. (b) Martinez, F. N.; Schlegel, H. B.; Newcomb, M. *J. Org. Chem.* **1996**, *61*, 8547−8550.

(7) Dowd, P.; Zhang, W. *Chem. Rev.* **1993**, *93*, 2091−2115.

(8) (a) Beckwith, A. L. J. *Chem. Soc. Rev.* **1993**, 143−151. (b) Curran, D. P. Radical Cyclizations and Sequential Radical Reactions. In *Comprehensive Organic Synthesis*; Trost, B. M., Ed.; Permagon; Oxford, 1991; Vol. 4, Chapter 4.2, pp 779−831. (c) Giese, B. *Radicals In Organic Synthesis: Formation of Carbon−Carbon Bonds*; Permagon Press: Oxford, 1986.

10.1021/jo981708n CCC: $18.00
Published on Web 12/29/1998

Scheme 1

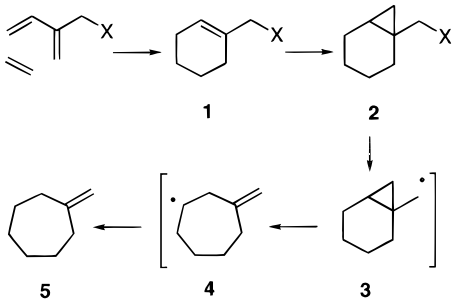

Scheme 2

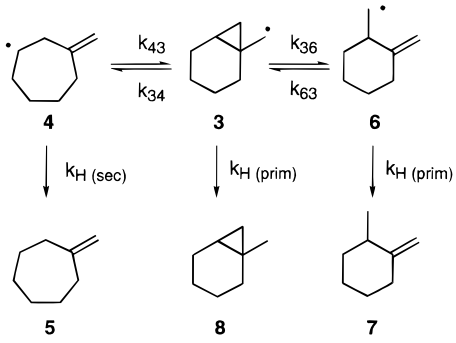

mental need to understand how stereoelectronic effects guide the outcome of radical reactions.

The cyclopropylcarbinyl → homoallyl radical transformation, when incorporated into a ring system (e.g., **3**, Scheme 2) has received far less attention than the acyclic analogues. In cases where the radical center of the cyclopropylcarbinyl moiety is embedded in the bicyclo[*n*.1.0] system, there tends to be a strong stereoelectronic preference for exocyclic ring opening.[10−12] The situation is quite different when the radical center is exo to the bicyclic ring system (e.g., **3**). Here increased conformational mobility of the radical-bearing center allows SOMO overlap with either of the β-cyclopropyl bonds; consequently, both homoallylic radicals **4** and **6** are accessible.[13,14]

Several factors come into play when attempting to predict which homoallylic radical will be formed from cyclopropylcarbinyl radical **3**. The incipient primary vs secondary radical character, the build-up of ring strain in the respective transition states, the relief of cyclopropyl substituent bond eclipsing interactions, and any inherent preference in the orientation of the SOMO of the initial radical **3** all constitute factors which may influence the outcome. Indeed, some of these variables have contradictory effects making a priori product distribution difficult to predict. A more thorough discussion of these factors is presented in the computational section of this paper.

Our previous studies[15] of radical **3** and other structural analogues indicated that seven-membered ring formation could be controlled to some extent by increasing the concentration of the reducing agent (an indication of kinetic control). As discussed in greater detail later in this paper, MP4/6-31G*//HF/6-31G* calculations indicated that ring expansion (ultimately providing methylenecycloheptane **5**) was kinetically favored over the nonexpansion route (leading to **7**) by 3.4 kcal/mol. On the basis of these insights we decided to pursue synthetic studies aimed at developing this novel methodology.

Synthesis and Kinetic Analysis. In initial studies, we employed the *S*-methylthiocarbonate (xanthate ester) derivative of the cyclopropyl alcohol as the radical precursor (**2**, X = OC(=S)SCH$_3$).[15] Regrettably, generation of the radical with this substrate called for forcing conditions (PhH, 135 °C, sealed tube reactor). This requirement precluded kinetic analysis over a conventional temperature range, and therefore a more versatile radical precursor was sought. In this regard, Barton's *N*-hydroxypyridine-2-(1*H*)-thione (PTOC, from pyridine-2-thione-*N*-oxycarbonyl) ester was an attractive alternative in that it proves capable of generating radicals across a wide range of temperatures.[16]

PTOC ester **12** was prepared in five steps as outlined in Scheme 3. Application of the Wadsworth−Emmons procedure[17] to cyclohexanone with triethylphosphonoacetate (NaH, THF) provided the unsaturated esters **9a**/**9b** in 73% yield as a 52:48 mixture of the β,γ:α,β isomers (capillary GC). The desired β,γ-unsaturated ester **9b** could be prepared quantitatively from the crude mixture by kinetic trapping of the extended enolate (LDA, THF) with saturated aqueous NH_4Cl at −78 °C. Cyclopropanation with diethyl zinc/diiodomethane in either THF or Et_2O consistently failed to consume all of the alkene which complicated purification as the starting material and the cyclopropanated product have identical R_f values on TLC. When dichloromethane was employed, however,

(9) For a recent example see: Jung, M. E.; Rayle, H. L. *J. Org. Chem.* **1997**, *62*, 4601−4609.

(10) For examples, see (a) Batey, R. A.; Grice, P.; Harling, J. D.; Motherwell, W. B.; Rzepa, H. S. *J. Chem. Soc., Chem. Commun.* **1992**, 942−944. (b) Clive, D. L. J.; Daigneault, S. *J. Org. Chem.* **1991**, *56*, 3801−3814. (c) Friedrich, E. C.; Holmstead, R. L. *J. Org. Chem.* **1972**, *37*, 2546−2550. (d) Friedrich, E. C.; Holmstead, R. L. *J. Org. Chem.* **1972**, *37*, 2550−2554. (e) Batey, R. A.; Harling, J. D.; Motherwell, W. B. *Tetrahedron* **1992**, *48*, 8031−8052. (f) Harling, J. D.; Motherwell, W. B. *J. Chem. Soc., Chem. Commun.* **1988**, 1380−1382. (g) Davies, A. G.; Muggleton, B.; Godet, J.-Y.; Pereyre, M.; Pommier, J.-C. *J. Chem. Soc., Perk. Trans. 2* **1976**, 1719−1724. (h) Boikess, R. S.; Mackay, M.; Blithe, D. *Tetrahedron Lett.* **1971**, 401−404. (i) Clive, D. L. J.; Daigneault, S. *J. Org. Chem.* **1991**, *56*, 5285−5289. (j) For an example of a nine-membered ring, see Thies, R. W.; McRitchie, D. D. *J. Org. Chem.* **1973**, *38*, 112−116. (k) For an example where SmI_2 is used to generate a ketyl radical adjacent to a cyclopropyl ring, see Batey, R. A.; Motherwell, W. B. *Tetrahedron Lett.* **1991**, *32*, 6649−6652.

(11) Ingold, K. U.; Walton, J. C. *Acc. Chem. Res.* **1986**, *19*, 72−77.

(12) The yield of the ring-expanded product typically is 0−10% in these cases; however, exceptions have been reported: see refs 10a and 13c.

(13) For cyclopentyl analogues, see (a) Beckwith, A. L. J.; O'Shea, D. M. *Tetrahedron Lett.* **1986**, *27*, 4525−4528. (b) Stork, G.; Mook, R., Jr. *Tetrahedron Lett.* **1986**, *27*, 4529−4532. (c) Green, S. P.; Whiting, D. A. *J. Chem. Soc., Chem. Commun.* **1992**, 1754−1755. (d) Beckwith, A. L. J.; Phillipou, G. *Chem. Commun.* **1971**, 658−659. (e) Cristol, S. J.; Barbour, R. V. *J. Am. Chem. Soc.* **1968**, *90*, 2832−2838. (f) Destabel, C.; Kilburn, J. D. *J. Chem. Soc., Chem. Commun.* **1992**, 596−598.

(14) A system similar to **3** has been reported: Dauben, W. G.; Shaffer, G. W.; Deviny, E. J. *J. Am. Chem. Soc.* **1970**, *92*, 6273−6281. Here, photoexcitation of **I** led to the ring-expanded 1-acetylcycloheptene (**II**), but under the conditions of the experiment, the product isolated was primarily the dimerized material.

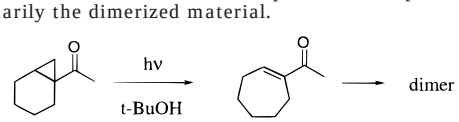

(15) Kantorowski, E. J.; Borhan, B.; Nazarian, S.; Kurth, M. J. *Tetrahedron Lett.* **1998**, *39*, 2483−2486.

(16) Barton, D. H. R.; Crich, D.; Motherwell, W. B. *Tetrahedron* **1985**, *41*, 3901−3924.

(17) Wadsworth, W. S., Jr.; Emmons, W. D. *Org. Syntheses*; Wiley: New York, 1963; Vol. IV, pp 547−549.

(18) (a) Takahashi, H.; Yoshioka, M.; Ohno, M.; Kobayashi, S. *Tetrahedron Lett.* **1992**, *33*, 2575−2578. (b) McDonald, W. S.; Verbicky, C. A.; Zercher, C. K. *J. Org. Chem.* **1997**, *62*, 1215−1222.

Scheme 3

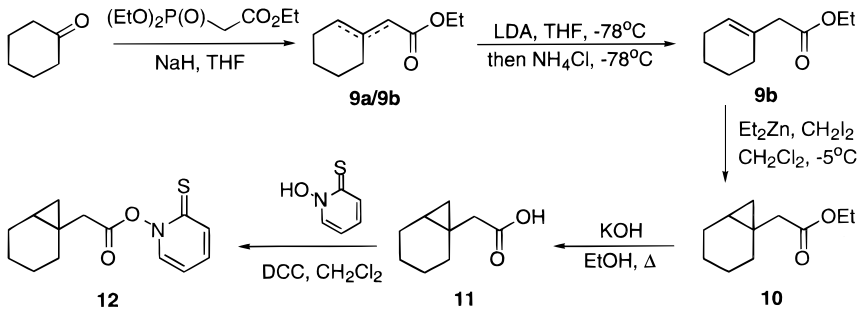

ester **10** was produced in 86−92% yield with no evidence of **9b**.[18] Saponification of ester **10** in KOH/EtOH followed by subsequent acidification afforded the cyclopropyl acid **11** in 92% yield. Radical precursor **12** was then prepared by DCC coupling of acid **11** with 2-mercaptopyridine *N*-oxide. This PTOC ester, isolated as a yellow solid, is stable for weeks in air if protected from light, but slowly decomposes when left as a solution in THF or $CDCl_3$.

Radical **3** is generated from PTOC ester **12** in THF by irradiation with visible light in the presence of either tributylstannane or thiophenol. The reaction is facile (typically under 60 s) and, for the stannane reactions, can be readily visualized by the loss of solution color (yellow → colorless).[19] The reaction products were analyzed by capillary GC, and yields were determined using a hydrocarbon internal standard. Authentic reaction products **5** and **7** were prepared by Wittig olefination of the corresponding ketones. 1-Methylbicyclo[4.1.0]heptane (**8**) was prepared by dehydration of 1-methylcyclohexanol followed by cyclopropanation (Et_2Zn, CH_2I_2, CH_2Cl_2).

The cyclopropylcarbinyl radical **3** was analyzed across a temperature range of −75 °C to 59 °C. Both thiophenol and tri-*n*-butylstannane were used in >10 equiv for all reactions in order to apply pseudo-first-order approximations for kinetic analyses. Thiophenol concentration varied between 0.4 and 1.25 M; tri-*n*-butylstannane concentration varied between 0.2 and 0.8 M. In all cases, lower temperatures and higher concentrations of reducing agent favored the ring-expanded product **5** over the nonexpanded product **7**. The combined yields (GC; internal hydrocarbon standard) of **5**, **7**, and **8** ranged between 96 and 98% when thiophenol was employed and 94−98% with tri-*n*-butylstannane. The chromatogram traces of the reactions were exceptionally clean for both of these reducing agents.

In general, thiols are excellent agents for trapping alkyl radicals with k_H approximately 1 order of magnitude faster than *n*-Bu_3SnH. Thiophenol, being especially fast, was used to establish the rates of ring opening of radical **3** for the two reaction pathways. The rate constant for the reaction between primary radicals **3** or **6** and thiophenol ($k_{H(prim)}$ in Scheme 2) was taken to be equal to the rate for the reduction of *n*-butyl radical by thiophenol (log $k_{H(prim)}/(M^{-1}s^{-1}) = 9.40-1.74/\theta$, $\theta = 2.303RT$).[20] The rate constant for the reaction between secondary radical **4** and thiophenol ($k_{H(sec)}$) was taken to be equal to the rate for the reduction of isopropyl radical by thiophenol (log $k_{H(sec)}/(M^{-1}s^{-1}) = 9.26-1.70/\theta$). At 25 °C this corresponds to reaction rates of 1.33×10^8 and 1.03×10^8, respectively.

(19) Also confirmed by TLC analysis.

(20) Franz, J. A.; Bushaw, B. A.; Alnajjar, M. S. *J. Am. Chem. Soc.* **1989**, *111*, 268−275.

Table 1. Product Distribution from Reduction of 12 in the Presence of PhSH

		relative % yield				
T (°C)	$[PhSH]_m$[a]	**5**	**8**	**7**	log k_{34}[b,c]	log k_{36}[d,e]
59	1.00	63.2	17.1	19.7	8.82	8.32
23	1.00	48.8	37.2	14.0	8.23	7.69
14	1.00	42.1	46.5	11.5	8.03	7.47
2	0.40	54.5	31.3	14.1	7.86	7.27
2	0.85	41.8	47.1	11.1	7.89	7.32
2	1.00	39.1	50.1	10.8	7.91	7.36
2	1.25	35.7	53.7	10.9	7.93	7.42
−22	1.00	20.6	73.7	5.7	7.33	6.77
−42	1.00	14.6	81.0	4.3	7.01	6.48
−75	1.00	5.2	92.5	2.4	6.28	5.94

[a] A stock solution of 0.02 M **12** was used for all runs. [b] From eq 1. [c] The value for $k_{H(sec)}$ was taken from reference 20 and equals the rate of the reaction between PhSH and isopropyl radical: $\log(k/(M^{-1}s^{-1})) = 9.26 - 1.70/\theta$, $\theta = 2.303RT$ in kcal/mol. [d] From eq 2. [e] The value for $k_{H(prim)}$ was taken from reference 20 and equals the rate of the reaction between PhSH and *n*-butyl radical: $\log(k/(M^{-1}\ s^{-1})) = 9.40 - 1.74/\theta$.

These are reasonable assumptions to make as the rate constants for the reactions between thiophenol and simple alkyl radicals are only slightly affected by the structure of the radical.[21] It has been shown that tin, sulfur, selenium, phosphorus, silicon, germanium, and carbon-centered radicals all participate in the chain process with PTOC esters. The rate at which any of the carbon-centered radicals formed in this process are intercepted by the starting ester is too slow to be of consequence when employing PhSH.[22] The rate for rearrangement of **3** → **4** is shown in eq 1, the rate for **3** → **6** in eq 2; where **5**/**8** and **7**/**8** represent the ratio of products (determined by GC), and $[PhSH]_m$ is the average concentration during the course of the reaction.

$$k_{34} = k_{H(sec)}[PhSH]_m\mathbf{5/8} \quad (1)$$

$$k_{36} = k_{H(prim)}[PhSH]_m\mathbf{7/8} \quad (2)$$

The results for PhSH reduction are shown in Table 1 and displayed graphically in Figure 1. The rate expressions derived from the Arrhenius plot are $\log(k_{34}/(s^{-1})) = (12.38 \pm 0.20) - (5.63 \pm 0.23)/\theta$ and $\log(k_{36}/(s^{-1})) = (11.54 \pm 0.32) - (5.26 \pm 0.37)/\theta$. At 298 K the rates for the unimolecular rearrangements of **3** → **4** and **3** → **6** are 1.78×10^8 s^{-1} and 4.90×10^7 s^{-1}, respectively. *Thus, at*

(21) The cyclopropylcarbinyl radical substructure of **3**, due to a resonance component which provides additional stabilization, may not react at a rate equal to that of *n*-butyl radical. For a commentary, see footnote 12 in Newcomb, M.; Glenn, A. G. *J. Am. Chem. Soc.* **1989**, *111*, 275−277.

(22) Newcomb, M.; Kaplan, J. *Tetrahedron Lett.* **1987**, *28*, 1615−1618.

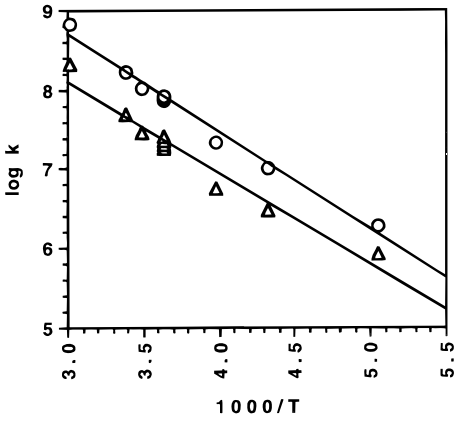

Figure 1. Arrhenius plots for the rearrangement of **3** → **4** (○) and **3** → **6** (△).

Table 2. Product Distribution from Reduction of 12 with Bu_3SnH

T (°C)	$[Bu_3SnH]_m$	**5**/**7**	*T* (°C)	$[Bu_3SnH]_m$	**5**/**7**
2	0.80	4.09	38	0.60	3.40
2	0.60	3.98	38	0.40	3.25
2	0.40	3.91	38	0.20	3.04
2	0.20	3.64	58	0.80	3.37
23	0.60	3.88	58	0.60	3.18
23	0.40	3.67	58	0.40	3.01
23	0.20	3.59	58	0.20	2.72

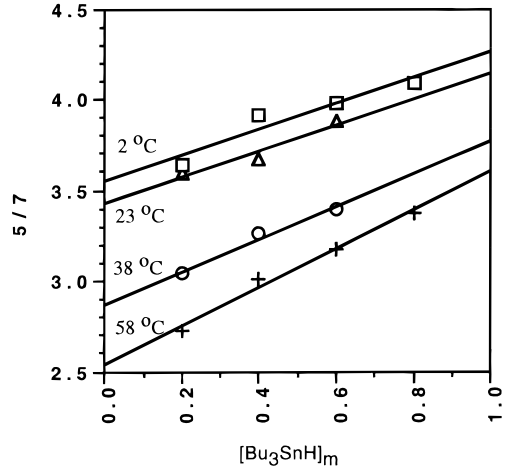

Figure 2. Product distribution of 5 and 7 using Bu3SnH.

*298 K the seven-membered ring radical **4** is formed 3.64 times faster than the nonexpanded radical **6**.*

We postulated that by employing a slower trapping agent it would be possible to allow radicals **3**, **4**, and **6** to partially equilibrate and thereby permit calculations relating to the reverse process of the cyclopropyl fragmentation. Hence, tri-*n*-butyltin hydride (which has rate constants on the order of 10^6 for simple aliphatic radicals) was used across various concentrations and temperatures to study the product distribution under equilibrating conditions. The fragmentation of the cyclopropylcarbinyl radical **3** is sufficiently fast (vide supra) that trapping by Bu_3SnH is a rare event, and, hence, alkenes **5** and **7** are primary products. The product ratios of **5** vs **7** are presented in Table 2. Figure 2 displays the results for the four isothermal reductions of radical precursor **12** at various concentrations of Bu_3SnH.

Subjecting Scheme 2 to kinetic steady-state analysis gives the product distribution of the two rearrangement products **5** and **7** as expressed in eq 3. The terms $k_{H(prim)}$ and $k_{H(sec)}$ refer to the rate of reduction by Bu_3SnH of a primary and secondary alkyl radical, respectively. The reported values are $\log(k_{H(prim)}/(M^{-1}\ s^{-1})) = 9.1 - 3.7/\theta$ for the reaction between Bu_3SnH and *n*-butyl radical; $\log(k_{H(sec)}/(M^{-1}\ s^{-1})) = 8.7 - 3.5/\theta$ for the reaction between Bu_3SnH and isopropyl radical.[23] At 25 °C $k_{H(prim)} = 2.4 \times 10^6\ M^{-1}\ s^{-1}$ and $k_{H(sec)} = 1.4 \times 10^6\ M^{-1}\ s^{-1}$. Furthermore, k_{36} and k_{34} are available from the thiophenol experiments.

$$\frac{\mathbf{5}}{\mathbf{7}} = \frac{k_{H(sec)}k_{34}}{k_{H(prim)}k_{36}} \times \frac{k_{63} + k_{H(prim)}[Bu_3SnH]_m}{k_{43} + k_{H(sec)}[Bu_3SnH]_m} \qquad (3)$$

In the event that both of the reverse reactions (i.e., **6** → **3** and **4** → **3**) are fast with respect to the rate of quenching (i.e., $k_{63} \gg k_{H\ (prim)}[Bu_3SnH]_m$ and $k_{43} \gg k_{H\ (sec)}[Bu_3SnH]_m$) then eq 3 simplifies to eq 4. Hence, the product distribution is proportional to the ratio of the rate constants for the reverse processes. This analysis, however, does not directly reveal whether the initial assumption of the reverse processes being rapid was correct. To ascertain this information, we start by allowing only one of the reverse processes to be fast relative to trapping by the reducing agent. Starting with the assumption that $k_{43} \gg k_{H\ (sec)}[Bu_3SnH]_m$, eq 3 becomes eq 5 which can be rearranged to the linear form as eq 6.

$$\frac{\mathbf{5}}{\mathbf{7}} = \frac{k_{H(sec)}k_{34}}{k_{H(prim)}k_{36}} \times \frac{k_{63}}{k_{43}} \qquad (4)$$

$$\frac{\mathbf{5}}{\mathbf{7}} = \frac{k_{H(sec)}k_{34}}{k_{H(prim)}k_{36}} \times \frac{k_{63} + k_{H(prim)}[Bu_3SnH]_m}{k_{43}} \qquad (5)$$

$$\frac{\mathbf{5}}{\mathbf{7}} = \frac{k_{H(sec)}k_{34}k_{63}}{k_{H(prim)}k_{36}k_{43}} + \frac{k_{34}k_{H(sec)}}{k_{36}k_{43}}[Bu_3SnH]_m \qquad (6)$$

The slope contains the rate of production of radical **3** from **4**, and the ratio of the intercept to the slope provides information about the rate of the production of radical **3** from **6**. Thus, each isotherm generated values for the rate of k_{43} and k_{63}. Using eq 6, the rate constants k_{43} and k_{63} were calculated at 25 °C and found to be $6.03 \times 10^6\ s^{-1}$ and $9.55 \times 10^6 s^{-1}$, respectively. These values are of similar magnitude to $k_H[Bu_3SnH]_m$ which implies that simplification of eq 3 to eq 5 is not valid. Therefore extraction of good values of k_{43} and k_{63} is not possible with this simple analysis. We therefore conclude that the rates of reverse reactions k_{43} and k_{63} are on the same order or slower than the reaction between Bu_3SnH and simple alkyl radicals ($\sim 10^6$).

As a secondary approach to analyzing the thermokinetics of this system, we decided to prepare PTOC ester **16** which would allow for direct generation of radical **6**. The commercially available methyl 1-cyclohexene-1-carboxylate was reduced with diisobutylaluminum hydride[24] in THF to afford the known[25] allylic alcohol **13** in 68% yield (Scheme 4). Acylation with acetic anhydride gave ester **14** in 84%, and subsequent Ireland−Claisen rearrangement[26] of the TMS ketene acetal of **14** provided

(23) Johnston, L. J.; Lusztyk, J.; Wayner, D. D. M.; Abeywickreyma, A. N.; Beckwith, A. L. J.; Scaiano, J. C.; Ingold, K. U. *J. Am. Chem. Soc.* **1985**, *107*, 4594−4596.
(24) Yoon, N. M.; Gyoung, Y. S. *J. Org. Chem.* **1985**, *50*, 2443−2450.
(25) Majetich, G.; Song, J.-S.; Ringold, C.; Nemeth, G. A.; Newton, M. G. *J. Org. Chem.* **1991**, *56*, 3973−3988.

Scheme 4

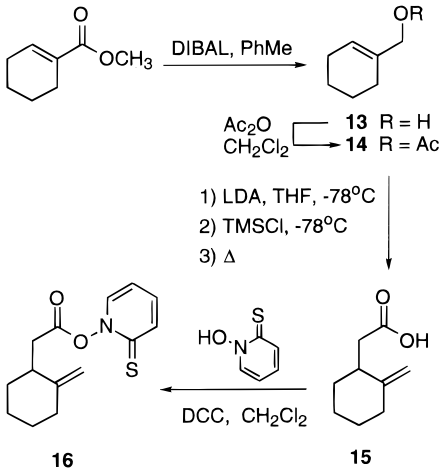

carboxylic acid **15** in 70%. In the absence of TMSCl, this rearrangement fails. Heating the reaction is also critical since, when conducted at room temperature, the product isolated is mainly the TMS ketene acetal. DCC coupling of carboxylic acid **15** and 2-mercaptopyridine *N*-oxide provided the PTOC ester **16** in 82% yield.

Radical generation from PTOC ester **16** was carried out with [Bu_3SnH] ≤ 0.10 M at 0, 23, and 53 °C. In all cases, no evidence of seven-membered ring product was detected (capillary GC). These results can be understood in terms of the origin of the radical precursor. The radical formed from **16** is not in the same conformation as the radical formed from rearrangement of **3**. Along the reaction coordinate for the rearrangement of **3** → **6**, the cyclohexane ring maintains a twist boat conformation as shown later in the computational section. This effect would not manifest itself for the cyclopentyl analogue of radical **3**. Stork,[13b] having generated the bicyclo[3.1.0]-hexanylcarbinyl radical from the corresponding bromide, observed a 4:1 ratio of the ring-expanded product over the nonexpanded product. Hence, as would be expected, the five-membered ring does not suffer the same conformational nuances that are associated with the cyclohexane-based system. The radical generated from **16**, which would generally occupy a chair conformation, must first adopt a twist boat conformation before cyclopropane **3** can be formed. Since this is energetically unfavorable, radical **6** (derived from **16**) fails to rearrange and is quenched, providing **7**.

Computational Analysis

By virtue of the relative insensitivity of radical processes to solvent effects, we thought these systems ideal for theoretical study. In support of this viewpoint are the papers by Schlegel and Newcomb,[6] wherein computational studies of several substituted cyclopropylcarbinyl radicals were performed. They determined that good structural data can be attained by using a UHF/6-31G* optimization. Higher level single point calculations were used to achieve acceptable agreement with experimental kinetic parameters, though the PMP2/6-31G*//UHF/6-31G* level of theory provided adequate descriptions of relative rate constants in their study.

(26) Ireland, R. E.; Mueller, R. H.; Willard, A. K. *J. Am. Chem. Soc.* **1976**, *98*, 2868−2877.

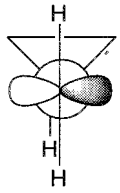

Figure 3. Newmann projection of cyclopropylcarbinyl radical.

As briefly mentioned earlier, a stereoelectronic prediction of the outcome of the cyclopropyl bond fragmentation in radical **3** is not easily derived from simple criteria. It is unclear which cyclopropyl bond will have best overlap with the radical p-orbital. Singly occupied p-orbitals in cyclopropylcarbinyl radicals generally orient themselves to best overlap with both vicinal cyclopropyl σ-bonds (Figure 3).[27,28] This is readily explained when one considers that a significant portion of the electron density for a cyclopropyl bond is displaced outside the internuclear axis. This extension of the bonding orbitals beyond the skeletal confines of the ring places them in good position to overlap with the radical p-orbital, thereby allowing a degree of delocalization of the radical into the cyclopropane ring.[29] This electronically favored orientation of the p-orbital offers no stereoelectronic differentiation between the two cyclopropyl σ-bonds.[30]

In the absence of definitive stereoelectronic differentiation, it was hoped that radical stability would influence the product distribution in our system. The process of **3** → **4** yields a thermodynamically more stable secondary radical from a primary radical (primary → secondary); whereas **3** → **6** yields a primary radical and no net stabilization of the radical center (primary → primary). The stability of the radical in the products could be expected to influence the thermodynamic product distribution. Additionally, it was hoped that the nascent secondary radical would help stabilize the transition state leading to the ring-expanded intermediate **4**.[31]

Opposing the potential stabilizing effect of the secondary radical is the increased ring strain of seven-membered ring **4** as opposed to six-membered ring **6**. This could favor product **6** thermodynamically. The degree to which strain energies could have a significant kinetic effect would depend on whether the transition state is product- or reactant-like; the former would be influenced more strongly by ring strain. It was evident to us from the preceding analysis that the question of kinetic and thermodynamic product distribution was not readily predicted. Hence, at the outset of developing this meth-

(27) (a) Cremer, D.; Kraka, E. *J. Am. Chem. Soc.* **1985**, *107*, 3800−3801. (b) de Meijere, A. *Angew. Chem., Int. Ed. Engl.* **1979**, *18*, *8*, 809−826. (c) Danen, W. C. *J. Am. Chem. Soc.* **1972**, *14*, 4835−4845.

(28) Although the term σ-bond will generally be used in this discussion in reference to the cyclopropyl skeletal bonds, it is generally acknowledged that these bonds actually incorporate p- as well as s-character.

(29) An alternative view presents itself in the realization that the orbitals which combine to form the cyclopropane σ-bonds have a high degree of p-character, thereby affording good p−p overlap with the radical p-orbital.

(30) Other factors, assuredly, can modify this ideal situation.

(31) Though it has been previously suggested for relatively simple systems that build-up of negative charge at the forming radical center in the transition state kinetically favors the primary radical product over the secondary (see ref 2b), our calculations indicate a partial positive charge on the incipient secondary radical center on **TS4** which, regardless of steric effects discussed later, should be stabilized by its secondary nature.

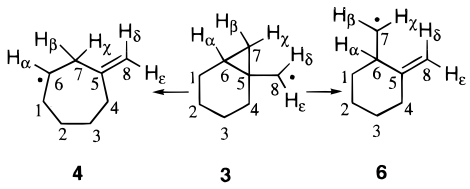

4 **3** **6**

Figure 4. Numbering scheme for intermediates **3**, **4**, and **6**. The same numbering scheme is used for **TS4** and **TS6**.

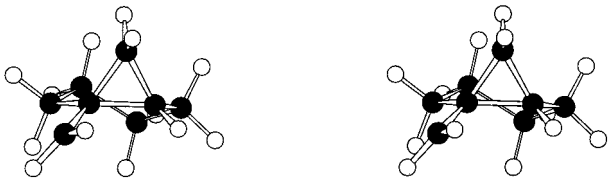

Figure 5. Stereo representation of the UHF/6-31G*-optimized geometry for the cyclopropylcarbinyl radical 3; note the symmetry of the cyclopropane ring.

odology, we undertook a theoretical investigation in parallel with our experimental studies.

Computational Results and Discussion

Initial starting guess geometries were generated using both Biosysm's Insight II Builder[32] module and Spartan[33] software. Preliminary semiempirical and HF/3-21G optimizations were conducted with Spartan software. All higher level optimizations and single point calculations were undertaken using Gaussian 92 and Gaussian 94 software packages.[34] All HF/6-31G* equilibrium and transition structures[35] were subjected to vibrational analysis to verify their natures and to acquire zero point vibrational data.[36] Figure 4 indicates the numbering scheme used in this discussion.

We first examined cyclopropyl radical **3** since it is the common starting point leading to both the expanded seven-membered carbocycle **4** as well as cyclopropyl-opened intermediate **6**. Scrutinizing Figure 5, one notes the near equilateral triangle of the cyclopropane ring. Figure 6 shows the very slight pyramidization of radical center C8. Contrary to the geometry expected from the prototypical system (Figure 3), we note the geometry of the carbinyl group provides better overlap with the β C5−C6 bond (Figure 6), though the reason for this geometric preference is not obvious. The relatively small enhancement of the overlap density between C5−C6 (0.280 e$^-$) vs C5−C7 (0.243 e$^-$) (Table 3) does not seem to indicate

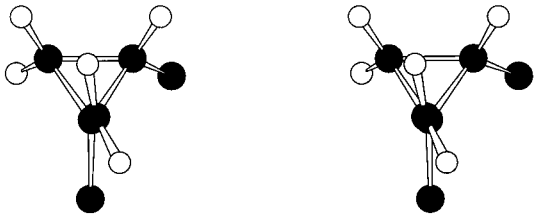

Figure 6. Stereo representation of the carbinyl geometry in 3; the view is along the C8−C5 bond (cf. Figure 3). The majority of the cyclohexane ring atoms have been removed for clarity. The unsubstituted carbon atoms correspond to C4 (bottom) and C1 (top right).

Table 3. Electron Overlap Density (e$^-$)[a]

atoms	4	TS4	3	TS6	6
1,2	0.337	0.346	0.342	0.338	0.329
2,3	0.325	0.335	0.338	0.338	0.331
3,4	0.334	0.339	0.347	0.344	0.337
4,5	0.355	0.343	0.364	0.351	0.356
5,6	−	*0.0678*	**0.280**	0.330	0.359
1,6	0.340	0.313	0.320	0.329	0.355
6,7	0.332	0.228	0.194	0.258	0.324
5,7	0.336	0.290	**0.243**	*0.00668*	−
5,8	**0.665**	*0.471*	**0.356**	*0.477*	**0.669**

[a] Italic type indicates bond order modification in the transition state. Bold type indicates sites of significant bond order modification in equilibrium structures.

Table 4. Selected Fermi Contact Analysis Data (atomic units) MP3/6-31G*//UHF/6-31G*[a]

atoms	4	TS4	3	TS6	6
1	−0.0501	−0.0286	0.0027	0.0045	0.0195
2	0.0525	0.0277	0.0020	0.0001	−0.0017
3	−0.0060	−0.0110	−0.0021	−0.0028	0.0046
4	0.0079	0.0240	0.0079	0.0249	−0.0093
5	0.0091	*−0.1135*	−0.0669	*−0.1074*	0.0467
6	**0.2412**	*0.1753*	0.0602	−0.0017	−0.0571
7	−0.0373	−0.0001	0.0245	*0.1579*	**0.2339**
8	0.0405	*0.1755*	**0.2166**	*0.1747*	−0.0350

[a] Bold type indicates predominantly localized radical center. Italic type indicates delocalization in the transition state.

sufficient additional electron density to account for this geometry, nor does the potential torsional interaction between the rather undemanding C8−H$_\epsilon$ and C4−C5 σ-bonds. Though an explanation for the geometry of the carbinyl radical center is not readily at hand, its effects are apparent in the form of hyperconjugation as expressed as a function of spin distribution.

Using Fermi contact analysis data as a gauge of the molecular spin distribution (Table 4), it is apparent that the predominant expression of the radical character for **3** is on C8, with an unpaired spin value of 0.2166 au. The hyperconjugation of the radical into adjacent cyclopropane σ-bonds is evident in the magnitude of the unpaired spin on the nuclei of C5, C6, and C7, the atoms encompassing the vicinal cyclopropyl bonds. The values of −0.0669, 0.0602, and 0.0245 au, respectively, show a degree of radical character unmatched by other carbon nuclei in the molecule. The reduced radical character on C7 indicates the relatively poor overlap of the singly occupied p-orbital with the C5−C7 σ bond. It is also of interest to note that only a modest enhancement of the unpaired spin on nucleus C4 is exhibited, affirming that bond C4−C5 is not in proper orientation to attain good overlap with the singly occupied p-orbital on C8.

From cyclopropyl radical **3**, two paths present themselves with the kinetically favored path leading to

(32) InsightII ver 3.2.0 Biosym Technologies Inc. 9685 Scranton Rd., San Diego, CA 92121-2777.

(33) Spartan SGI version 3.1.2 G Wave function Inc. 18401 Von Karman Suite 370, Irvine, CA 92715

(34) (a) Frisch, M. J.; Trucks, G. W.; Head-Gordon, M.; Gill, P. M. W.; Wong, M. W.; Foresman, J. B.; Johnson, B. G.; Schlegel, H. B.; Robb, M. A.; Replogle, E. S.; Gomperts, R.; Andres, J. L.; Raghavachari, K.; Binkley, J. S.; Gonzalez, C.; Martin, R. L.; Fox, D. J.; Defrees, D. J.; Baker, J.; Stewart, J. J. P.; Pople, J. A. Gaussian 92, Revision A. Gaussian, Inc., Pittsburgh, PA, 1992. (b) Frisch, M. J.; Trucks, G. W.; Schlegel, H. B.; Gill, P. M. W.; Johnson, B.; Montgomery, J. A.; Raghavachari, K.; Al-Laham, M. A.; Zakrzewski, V. G.; Challacombe, M.; Peng, C. Y.; Ayala, P. Y.; Chen, W.; Wong, M. W.; Andres, J. L.; Replogle, E. S.; Gomperts, R.; Martin, R. L.; Fox, D. J.; Binkley, J. S.; Defrees, D. J.; Baker, J.; Stewart, J. P.; Head-Gordon, M.; Gonzalez, C.; Pople, J. A. Gaussian 94. Gaussian, Inc. Pittsburgh, PA, 1995.

(35) HF/6-31G*//HF/6-31G* imaginary frequencies for **TS4** = −709.9289 cm^{-1}, for **TS6** = −716.2755 cm^{-1}.

(36) All zero point energies used in calculating the reported zero point corrected energy values have been subjected to the standard 0.89 frequency scaling factor.

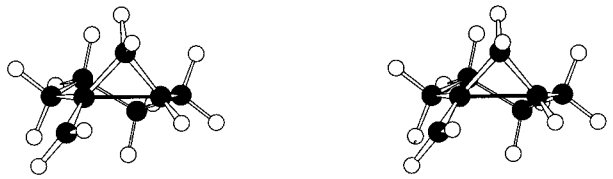

Figure 7. Stereo representation of the UHF/6-31G*-optimized geometry for **TS4**; note C5−C6 bond extension.

Table 5. C−C Bond Lengths (Å) UHF/6-31G*[a]

atoms	4	TS4	3	TS6	6
1,2	1.541	1.534	1.532	1.533	1.542
2,3	1.536	1.528	1.528	1.527	1.543
3,4	1.539	1.535	1.531	1.532	1.531
4,5	1.520	1.520	1.525	1.524	1.517
5,6	*2.477*	**1.871**	1.525	1.500	1.527
1,6	1.502	1.511	1.529	1.537	1.537
6,7	1.509	1.484	1.496	1.444	1.509
5,7	1.519	1.490	1.504	**1.889**	*2.515*
5,8	1.325	1.407	1.480	1.403	1.322

[a] Bold type indicates breaking bonds. Italic type indicates nonbonded C−C distances.

Table 6. Selected Bond Angles (deg) UHF/6-31G*

atoms	4	TS4	3	TS6	6
1,6,7	120.9	122.6	120.6	118.7	111.6
1,6,H_α	117.9	118.4	114.5	111.8	107.8
5,6,7	−	51.2	59.7	78.6	111.9
5,7,6	109.8	77.9	61.1	51.1	−
H_β,7,6	110.4	116.2	117.8	120.8	119.6
H_β,7,Hχ	107.0	111.1	113.6	117.8	117.7
H_χ,7,6	109.8	116.4	118.6	120.1	120.2
4,5,6	−	112.1	118.2	119.4	115.6
4,5,7	118.1	119.7	119.1	111.6	−
6,5,7	−	50.9	59.2	50.3	−
7,5,8	121.0	120.6	117.2	114.0	−
H_δ,8,5	121.8	121.2	120.4	121.4	121.8
H_δ,8,Hϵ	116.4	117.3	117.6	117.3	116.4
H_ϵ,8,5	121.8	121.0	120.4	120.9	121.8

expanded radical **4**, as discussed below. The reaction coordinate leading to **4** passes through transition state **TS4** (Figure 7). A comparison of Figure 5 with Figure 7 immediately shows extension of the breaking bond from 1.525 Å in cyclopropyl radical **3** to 1.871 Å in **TS4**. Obscure in Figure 7, but manifest in Table 5, is the contraction of bond C5−C8, having progressed nearly 50% of the way from the 1.480 Å of the single bond of **3** to the double bond of **4** (1.325 Å). Most bond angles in stationary points **3**, **TS4**, and **4** offer little to describe progress along the reaction coordinate owing to the general lack of rehybridization[37] of the centers involved with bond making and breaking. The main exception to this is the C5−C7−C6 bond angle which shows the release of ring strain as the cyclopropane ring opens (Table 6). In **TS4**, bond angle C5−C7−C6 has progressed 34% along its 48.7° reorganization from 61.1° of the sp^5 orbital in **3** to 109.8° of the rehybridized sp^3 orbital in **4**. Progress toward **4** is also evident in the H_δ−C8−C5−C7 dihedral angle (Table 7) which is increasingly flattened in going from −23.1° in radical **3** to −3.8° in **TS4** and finally crossing over to 3.7° of the π bond in **4**.

As the gross structural reorganization is occurring (**3** → **4**) there are dramatic changes occurring in the electronic structure of the molecule. The radical, predominantly localized on C8 in **3**, has delocalized in **TS4** (Table 4, italics). The unpaired spin density in **TS4** is spread evenly among C5 (−0.1135 au), C8 (0.1755 au), and C6 (0.1753 au) indicating the transfer of the radical from C8 to C6. In carbocyclic intermediate **4**, the radical has relocalized on C6 (0.2412 au) as expected. The total overlap population between any two atoms provides a measure of bond strength (or bond order). The bold face entries in Table 3 highlight regions of bond reorganization in **TS4**. The small C5−C6 value of 0.0678 e^- indicates the breaking of the cyclopropyl bond in concert with the strengthening of the C5−C8 bond (0.471 e^-) toward the double bond in **4** (0.665 e^-); compare with 0.356 e^- for the single bond in **3**. The transformation of the bent bonds of the cyclopropane to the standard σ-bonds is also apparent in the overlap data: C5−C7 (0.243 e^- in **3**) → (0.290 e^- in **TS4**) → (0.336 e^- in **4**) as well as C6−C7 (0.194 e^- in **3**) → (0.228 e^- in **TS4**) → (0.332 e- in **4**).

Table 7. Selected Dihedral Angles (deg)

atoms	4	TS4	3	TS6	6
H_δ,8,5,6	−	53.9	44.6	4.2	−1.7
H_δ,8,5,7	3.7	−3.8	−23.1	−52.6	−
1,6,5,4	−4.4	0.30	−0.08	−22.0	−26.0

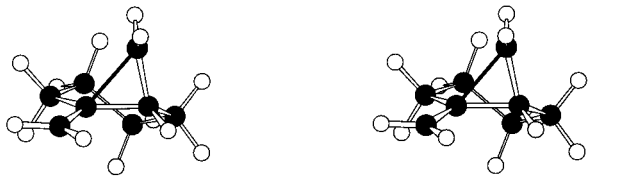

Figure 8. Stereo representation of the UHF/6-31G*-optimized geometry for **TS6**; note extension of the C5−C7 bond.

Traveling along the other branch of the reaction coordinate, **TS6** stands as counterpoint to **TS4**. The C5−C7 bond is in the process of breaking in **TS6** with an increased interatomic distance of 1.889 Å (Table 5). Figure 8 clearly shows this extension as a deviation from the symmetry of the cyclopropane ring in **3** (Figure 5). There are important electronic structure changes that occur with the accompanying geometric changes along the reaction pathway leading to **TS6** and product that parallel or contrast with the changes along the other reaction pathway. In the interest of manuscript brevity, however, we suppress discussion of these. They can be discerned in the data of Tables 3, 5, and 6 and Figure 8.

Much has already been said about the stationary points corresponding to **4** and **6**, in the preceding paragraphs. However, a brief discussion of their geometries is needed. These geometries represent the conformation achieved as the structures arrive along the reaction coordinate from their respective transition states, not necessarily the lowest energy conformations available for these structures. It is in this light that one should regard the conformations of these structures. The seven membered carbocyclic radical **4** is in an energetically favored chair-boat conformation (Figure 9), but the primary radical **6** is in a relatively high energy twist-boat conformation (Figure 10). To assess the thermodynamics of the reaction we have optimized the relaxed chair form of the radical, but it is of interest that the initial geometry coming off the reaction coordinate is a higher energy conformer.

The original ab initio calculations were undertaken using the 3-21G basis set, though as resources became

(37) C8 maintains its essential sp^2 character from radical in **3** to π-bond participant in **4**. Both C5 and C6 have sp^2-like character in the cyclopropane ring and are sp^2 hybridized in the product.

Figure 9. Stereo representation of the UHF/6-31G*-optimized geometry for **4**; note chair-boat conformation.

Figure 10. Stereo representation of the UHF/6-31G*-optimized geometry for **6**; note twist-boat conformation.

available, the structures were reoptimized using the 6-31G* basis set at the Hartree−Fock level of theory with a resulting moderate change in geometry and significant change in reaction parameters. All total energies calculated at levels of theory from UHF/3-21G through PMP4/6-31G* are reported in the supplemental data along with atomic spin densities and $\langle S^2 \rangle$ before and after projection of quartet contributions. Also included in the supplemental data are reaction energies along both reaction pathways and the differences of those parameters between the two pathways. We present here the more salient of these results (Tables 8, 9). It has been demonstrated[6a] that HF/6-31G*-optimized cyclopropylcarbinyl radical structures compared favorably with those optimized using the QCISD/6-31G* level of theory. This result lends credence to our choice of HF/6-31G* optimized structures for this study.

Single point calculations using second, third, and fourth order projected Møller−Plesset perturbation theory were conducted on HF/6-31G*-optimized structures to account for electron correlation. Theory appears to have converged at the MP2/6-31G*//HF/6-31G* level for relative reaction barriers with differences ranging to 0.4 kcal/mol (Table 9). Specific reaction parameters do not show so tight a convergence, with variations between levels of theory greater than 1 kcal/mol being common (Table 8). This is expected because spin contamination will have a greater effect on the elongated bonds of transition state structures.

Inspection of the E_{rxn} (**3** → **4**) − E_{rxn} (**3** → **6**) entries in Table 9 shows seven-membered carbocycle **4** to be both kinetically and thermodynamically favored regardless of level of theory or basis set. The zero-point energy corrected values for the energies of reaction show expanded radical intermediate **4** to be favored over cyclopropane-opened intermediate **6** by 1−2 kcal/mol. Yet these figures can be misleading. As noted above and evident in Figure 10 the optimized structure for radical **6** lies in a twist-boat conformation as dictated by the geometry of **TS6**. This is by no means the lowest energy conformer for such structures. For this reason we undertook a conformational search yielding the low energy chair conformation **6′** shown in Figure 11. As can be seen in Table 9, now the six-membered radical intermediate is unambiguously the thermodynamic product at all levels of theory, favored by 2.1 kcal/mol for the PMP4/6-31G*//HF/6-31G* calculation.

The geometries of the transition structures **TS6** and **TS4** are dictated by that of cyclopropylcarbinyl radical **3**, and therefore the calculated reaction barrier heights can be compared without regard to conformational analysis. In this light, scrutiny of Table 9 shows a kinetic bias of 3.0 kcal/mol for the formation of secondary cycloheptyl radical **4** as calculated via zero-point energy corrected PMP4/6-31G*//HF/6-31G* single point data. We focus on the PMP4 results because they are the highest level of correlation we have considered, and the spin projection removes contamination from higher multiplets and the artifacts they may contribute to the transition state energies. The spin contamination of the UHF calculations was very modest for the structures corresponding to potential surface minima. The $\langle S^2 \rangle$ values differed from the expected doublet value of 0.75 by at most 0.04. The contamination was almost entirely due to quartets, as removal of their contribution by projection reduced the maximum difference to 0.0009. As is common, the spin contamination for the two transition states was greater than that for the equilibrium structures. $\langle S^2 \rangle$ was 0.9418, 0.9578 for **TS4** and **TS6**, respectively. The transition state spin contamination was also dominated by quartets, for after they were removed by projection, $\langle S^2 \rangle$ reduced to 0.7567 and 0.7574, respectively. Removal of still higher spin states in preparation for the PMP energy calculations reduced $\langle S^2 \rangle$ to 0.75000 in all cases. Absolute barrier heights for the rearrangements **3** → **4** and **3** → **6** were calculated (PMP4/6-31G*//HF/6-31G* (Z)) to be 6.0 and 9.1 kcal/mol, respectively.[38] These data are in qualitative agreement with the experimentally determined reaction rates.

Several hypotheses have been suggested to account for kinetic regiochemistry observed in radical ring opening reactions of substituted cyclopropylcarbinyl radicals.[31,39] Of these, that championed by Schlegel and Newcomb[6] prove most aptly applied to carbinyl radical **3**. They explored the ring opening of a variety of methyl- and dimethyl-substituted cyclopropyl carbinyl radicals using ab initio techniques. They concluded that the rate and consequently the regiochemistry of ring opening was dramatically influenced by eclipsing interactions between the carbinyl group and a vicinal methyl group (Figure 12). Even though cyclopropylcarbinyl **3** does not offer such a steric interaction between the carbinyl group and a vicinal C−C bond, it does have an analogous eclipsing interaction between the two vicinal C−C bonds of the fused cyclohexane ring (C4−C5−C6−C1 dihedral = −0.80° (Table 7). Adjustments to minimize these eclipsing interactions are evident in both **TS4** (Figure 7) and **TS6** (Figure 8). In **TS4** the bonds are still essentially eclipsed (C4−C5−C6−C1 dihedral = 0.30°); nevertheless, the destabilizing effect of the eclipsed bonds is lessened by the increased distance between those bonds afforded by the lengthening of the C5−C6 cyclopropyl σ-bond (1.871 Å, Table 5). **TS6** exhibits a significant degree of torsional flexing from the near coplanar disposition of C4−C5−C6−C1 in **3**. The C4−C5−C6−C1 dihedral angle has opened to −22.0° in **TS6** allowing some relief from the eclipsing inherent in **3**. Yet the −22.0° dihedral of **TS6** or even the −26.0° dihedral of the twist-boat conformer of stationary point **6** is remote from the ideal gauche

(38) Ab initio calculation results in other cyclopropylcarbinyl radical systems indicate that though these calculations prove quite useful for relative barrier height comparisons, absolute barrier heights should be viewed with some caution (see ref 6a).

(39) Mariano, P. S.; Bay, E. *J. Org. Chem.* **1980**, *45*, 1763−1769.

Table 8. Reaction Parameters (kcal/mol)

calculation level	E_a **3** → **4**	E_a **3** → **6**	E_a **4** → **3**	E_a **6** → **3**	E_{rxn} **3** → **4**	E_{rxn} **3** → **6**	E_{rxn} **3** → **6′**
HF/6-31G*	10.5	13.5	16.1	15.7	−5.5	−2.3	−7.8
HF/6-31G* (Z)[a]	9.7	12.2	15.0	15.2	−5.3	−3.0	−8.3
MP4/6-31G*//HF/6-31G* (Z)[a]	11.1	14.6	12.6	14.4	−1.5	0.2	−4.9
PMP4/6-31G*//HF/6-31G* (Z)[a]	6.0	9.1	8.2	9.5	−2.2	−0.4	−5.1

[a] Zero-point energy-corrected values. Zero-point energies taken from HF/6-31G*-optimized structures and scaled by 0.89.

Table 9. Relative Reaction Barrier and Energy of Reaction Comparisons (kcal/mol)

calculation level	E_a(**3** → **6**) − E_a(**3** → **4**)	E_{rxn}(**3** → **4**) − E_{rxn}(**3** → **6**)	E_{rxn}(**3** → **4**) − E_{rxn}(**3** → **6′**)
HF/6-31G*	2.9	−3.3	2.3
HF/6-31yG* (Z)[a]	2.4	−2.3	3.0
MP4/6-31G*//HF/6-31G* (Z)[a]	3.4	−1.7	3.4
PMP4/6-31G*//HF/6-31G* (Z)[a]	3.0	−1.8	2.8

[a] Zero-point energy-corrected values. Zero-point energies taken from HF/6-31G*-optimized structures and scaled by 0.89.

Figure 11. Stereo representation of the PMP4/6-31G*//HF/6-31G*, optimized geometry for **6′**.

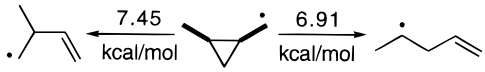

Figure 12. Reaction barriers for ring opening PMP2/6-31G*//HF/6-31G*, zeropoint corrected.[6a]

angle of 60.0°.[40] Breaking the C5−C6 bond in **TS4** appears to offer greater relief from the destabilizing eclipsing interactions than the partial bond rotation observed in **TS6**. Apparently, reduction of the eclipsing interaction in conjunction with the stabilizing effect of the incipient secondary radical in large part account for the PMP4/6-31G*//HF/6-31G* (Z) result (Table 9) indicating *path* ***3*** → ***4*** *is kinetically favored by 3.0 kcal/mol over* ***3*** → ***6***.

Cyclohexyl radical **6′** is calculated to be 2.1 kcal/mol more stable than cycloheptyl radical **4**; this can be rationalized on the grounds of ring strain and radical stability. Based purely on the ring strain of cyclohexanes vs cycloheptanes,[41] one would expect **6** to be favored by 6.3 kcal/mol. However, **6** is a primary radical while **4** is a secondary radical; this should stabilize **4** by roughly 3.5 kcal/mol[42] relative to **6**. Combining these opposing effects places **6** roughly 2.8 kcal/mol lower in energy than **4**. This rationalization gives a surprisingly good quantitative estimate in comparison with the calculated and experimental results.

In the kinetic analysis, E_a values taken from the Arrhenius expression suggests the two pathways are comparable (5.63 vs 5.26 kcal/mol). Taking the error bars into account reveals that **3** → **4** could be favored at one extreme by 0.23 kcal/mol and **3** → **6** at the other by 0.97 kcal/mol. This apparent ambiguity between which pathway is favored is resolved when one considers that the preexponential factor dominates for transformation **3** → **4** (12.38 vs 11.54). It is unrealistic to expect the accuracy of the theoretical methods employed in this study to exceed a few kcal/mol for energy of activation. The computations indicate that the activation barriers for formation of both products are very close, the experimental difference being less than a kcal/mol. Within the accuracy we can expect for this level of theory, there is consonance between the experimental activation energies and those calculated theoretically. We believe the qualitative aspects of the transition state structures to be the more important contribution from theory to our understanding of this reaction.

The quantitative aspects of the theoretical calculation of the change in entropy to the transition state are even less reliable than are the energetics. Still some enheartening aspects emerge. Kinetic and theoretical data provides $\Delta S^{\ddagger}$ (**3** → **4**) as −3.67 eu and −1.842 eu, respectively. Likewise, $\Delta S^{\ddagger}$ (**3** → **6**) is found to be −7.47 eu and −0.943 eu. A decrease in entropy is to be expected for both of these processes since the freely rotating methyl radical in **3** must adopt an orientation which allows for proper overlap with one of the cyclopropyl σ bonds. Progress along either pathway necessitates that the initial •CH_2 ultimately become locked into the fixed geometry of the resulting C=C bond. This ordering will certainly outweigh any additional degrees of freedom gained by the carbocycle as a result of loss of the fused cyclopropyl group.

Conclusion

Calculations and experimentation indicated that the rearrangement of radical **3** could be manipulated to favor two different products depending on three reaction parameters: temperature, concentration, and choice of the reducing agent. The more rigorous kinetic study presented in this paper showed that indeed radical **3** can be induced to give predominantly expanded product **5**. A general methodology coupling this radical ring expansion with the Diels−Alder cyclization will prove a potent synthetic tool.

Experimental Section

General Procedures. Solvents were purified as follows: tetrahydrofuran (THF) was distilled from sodium/benzophenone ketyl; methylene chloride (CH_2Cl_2) was distilled from CaH_2; benzene was distilled from potassium. All reactions, unless otherwise noted, were conducted under an inert atmosphere (N_2 or Ar). ^{1}H and ^{13}C NMR spectra were measured in $CDCl_3$ at 300 and 75 MHz, respectively, and chemical shifts are reported in ppm downfield from internal tetramethylsilane. Thin-layer chromatography (TLC) was performed on silica gel

(40) One should not discount the destabilizing effect on **TS6** of the partial adoption of the twist-boat conformation.

(41) Liebman, J. F.; Greenberg, A. *Chem. Rev.* **1976**, *76*, 311−353.

(42) From bond dissociation energies: Benson, S. W. *J. Chem. Educ.* **1965**, *42*, 502−518.

plates, and components were visualized by UV light, iodine, or by heating the plates after treatment with a phosphomolybdic acid reagent (1:1 in EtOH). CC, RC, and PC refer to column, radial, and planar chromatography on silica gel, respectively. For CC and RC the eluent indicated refers to the starting mixture of stepwise elution. Elemental analyses were performed at the MidWest Microlab, Indianapolis, IN.

Unsaturated Esters (9a/9b). The procedure described by Emmons was followed.[17] Vacuum distillation (62.0 °C at 1.0 mmHg) afforded a 52:48 mixture (per capillary GC) of the β,γ:α,β isomers (20.3 g; 73.1%; lit. yield 67−77%).

Ethyl 2-(1-Cyclohexenyl)acetate (9b). To a 0 °C solution of diisopropylamine (1.092 g, 10.79 mmol) in THF (40 mL) was slowly added *n*-butyllithium (7.1 mL, 1.48 M in hexanes). The solution was stirred for 20 min and then cooled to −78 °C. The mixture of esters **9a**/**9b** (1.68 g, 9.99 mmol) in THF (8 mL) was added dropwise over 10 min and allowed to stir for an additional 10 min. Saturated aqueous NH_4Cl (9 mL) was added dropwise over 10 min, and the quenched reaction was allowed to warm to ambient temperature, poured into H_2O (75 mL), and extracted with Et_2O (3 × 30 mL). The extracts were dried (Na_2SO_4), filtered, and concentrated to afford 1.68 g (9.99 mmol, 100%) of the β,γ-unsaturated ester **9b** as a colorless liquid. Capillary GC analysis showed no evidence of conjugated ester **9a**. FTIR (thin film) 3060 (weak), 1735 cm^{-1}. ^1H NMR δ 1.23 (t, 3H, J = 7.1 Hz), 1.52−1.65 (m, 4H), 1.97−1.99 (m, 4H), 2.90 (s, 2H), 4.10 (q, 2H, J = 7.1 Hz), 5.53 (s, 1H).

Ethyl 2-Bicyclo[4.1.0]heptylacetate (10). To a −5 °C solution of Et_2Zn (13.7 mL, 1.0 M in hexanes) in CH_2Cl_2 (50 mL) was added dropwise CH_2I_2 (7.37 g, 27.5 mmol) over 10 min. A white precipitate formed when the addition was approximately half complete. After an additional 10 min, ester **9b** (1.465 g, 8.71 mmol) in CH_2Cl_2 (8 mL) was added in one portion, and the reaction was allowed to stir at room temperature for 9 h during which time most of the white precipitate had dissolved. The reaction was poured into saturated aqueous NH_4Cl (200 mL) and extracted with Et_2O (2 × 150 mL). The combined organics were dried (Na_2SO_4), filtered, and concentrated. The crude material could be used without further purification. CC (5% EtOAc/hexanes) afforded the pure ester **10** as a colorless liquid (1.381 g, 87%). FTIR (thin film) 1736 cm^{-1}. ^1H NMR δ 0.25 (t, 1H, J = 5.0 Hz), 0.47 (dd, 1H, J = 9.2, 5.0 Hz), 0.78−0.86 (m, 1H), 1.06−1.33 (m, 4H), 1.24 (t, 3H, J = 7.1 Hz), 1.51−1.59 (m, 1H), 1.63−1.78 (m, 2H), 1.84−1.95 (m, 1H), 2.10 (d, 1H, J = 15.0 Hz), 2.22 (d, 1H, J = 15.0 Hz), 4.11 (q, 2H, J = 7.1 Hz). ^{13}C NMR δ 14.29, 16.56, 16.86, 17.66, 21.07, 21.52, 23.79, 28.72, 46.24, 59.91, 172.63.

2-Bicyclo[4.1.0]heptylacetic Acid (11). Ester **10** (0.554 g, 3.04 mmol) in basic EtOH (1.93 g KOH in 25 mL 95% EtOH) was heated at reflux for 2 h. The reaction was diluted with Et_2O and extracted with aqueous NaOH (2 M; 2 × 40 mL). The combined extracts were acidified with aqueous HCl and extracted with Et_2O (3 × 40 mL). The combined organics were dried (Na_2SO_4), filtered, and concentrated to give an orange liquid. CC (30% EtOAc/hexanes) afforded the pure acid **11** as a colorless liquid (0.431 g, 92%). FTIR (thin film) 2930 (br), 1706 cm^{-1}. ^1H NMR δ 0.29 (t, 1H, J = 5.0 Hz), 0.51 (dd, 1H, J = 9.2, 5.0 Hz), 0.80−0.88 (m, 1H), 1.09−1.34 (m, 4H), 1.52−1.60 (m, 1H), 1.66−1.84 (m, 2H), 1.86−1.97 (m, 1H), 2.22 (s, 2H), 11.90 (br s, 1H). ^{13}C NMR δ 16.31, 16.85, 17.73, 21.00, 21.44, 23.72, 28.65, 46.08, 179.53.

1-[2-(Bicyclo[4.1.0]heptyl)acetoxy]-2(1*H*)-pyridinethione (12). Carboxylic acid **11** (0.598 g, 3.88 mmol), 2-mercaptopyridine-*N*-oxide (0.494 g, 3.88 mmol), and DMAP (46.9 mg, 0.38 mmol) were dissolved in CH_2Cl_2 (50 mL). The reaction flask was covered with foil to protect it from light, and DCC (0.886 g, 4.29 mmol) in CH_2Cl_2 (15 mL) was added dropwise over 20 min. The bright yellow reaction mixture was allowed to stir for 10 h at ambient temperature. The dicyclohexylurea was filtered off, and the yellow filtrate was concentrated. CC (30% EtOAc in hexanes) provided 0.812 g (3.08 mmol, 79%) of the pure PTOC ester **12** as a yellow solid. mp = 106.0−107.0 °C. FTIR (KBr) 1804, 1531, 1136, 1062, 750 cm^{-1}. ^1H NMR δ 0.36 (t, 1H, J = 5.1 Hz), 0.59 (dd, 1H, J = 9.3, 5.1 Hz), 0.90−0.98 (m, 1H), 1.11−1.39 (m, 4H), 1.52−1.61 (m, 1H), 1.79−1.97 (m, 3H), 2.51 (d, 1H, J = 16.6 Hz), 2.66 (d, 1H, J = 16.6 Hz), 6.61 (td, 1H, J = 6.9, 1.6 Hz), 7.17 (ddd, 1H, J = 8.8, 6.9, 1.4 Hz), 7.54 (dd, 1H, J = 6.9, 1.4 Hz), 7.63 (dd, 1H, J = 8.8, 1.6 Hz). ^{13}C NMR δ 15.71, 16.94, 17.76, 20.71, 21.31, 23.48, 28.55, 43.36, 112.45, 133.38, 137.18, 137.66, 167.86, 175.71. Anal. Calcd for $C_{14}H_{17}NO_2S$: C, 63.85; H, 6.51; N, 5.32. Found: C, 63.78; H, 6.51; N, 5.42.

1-Cyclohexenylmethyl Acetate (14). To a 0 °C solution of 1-cyclohexenemethanol (**13**) (0.492 g, 4.39 mmol) and acetic anhydride (1.365 g, 13.16 mmol) in CH_2Cl_2 (15 mL) was added Et_3N (1.791 g, 17.70 mmol) and DMAP (59 mg, 0.48 mmol). The ice bath was removed, and the reaction was stirred at ambient temperature for 1.5 h. Methanol (5 mL) was added to quench the excess Ac_2O and, after a further 30 min at ambient temperature, the reaction was diluted with H_2O and extracted with CH_2Cl_2 (3 × 20 mL). The combined organics were dried (Na_2SO_4), filtered, and concentrated. CC (20% EtOAc in hexanes) afforded the allylic acetate **14** as a colorless liquid (0.569 g, 84.0%). FTIR (thin film) 1739, 1229, 1024 cm^{-1}. ^1H NMR δ 1.54−1.69 (m, 4H), 1.98−2.07 (m, 4H), 2.06 (s, 3H), 4.43 (s, 2H), 5.73 (br s, 1H). ^{13}C NMR δ 20.79, 21.97, 22.22, 24.85, 25.72, 68.77, 126.16, 132.74, 170.78.

2-(2-Methylenecyclohexyl)acetic Acid (15). To a 0 °C solution of diisopropylamine (0.187 g, 1.84 mmol, freshly distilled from NaOH) in THF (7 mL) was added slowly via syringe *n*-BuLi (1.19 mL, 1.44 M in hexanes). The solution was allowed to stir at 0 °C for 10 min and then cooled to −78 °C. A solution of the allylic acetate **14** (0.238 g, 1.54 mmol) in THF (2 mL) was added via syringe and then followed immediately by addition of TMSCl (0.21 mL, 1.65 mmol). The reaction was allowed to warm to room temperature and then refluxed for 12 h. After the reaction was cooled to room temperature, CH_3OH (5 mL) was added, the solution was stirred for 2 h, and the solution was diluted with Et_2O and extracted with aqueous 2 M NaOH (2 × 40 mL). The combined aqueous extracts were acidified with aqueous 2 M HCl and extracted with Et_2O (2 × 25 mL). The organic solution was washed with H_2O, dried (Na_2SO_4), filtered, and concentrated. CC (30% EtOAc in hexanes) afforded the pure acid **15** as a colorless liquid (0.165 g, 70%). FTIR (thin film) 2940 (br), 1708, 1646 cm^{-1}. ^1H NMR δ 1.14−1.27 (m, 1H), 1.32−1.56 (m, 2H), 1.68−1.77 (m, 2H), 1.80−1.88 (m, 1H), 2.01−2.09 (m, 1H), 2.26−2.32 (m, 1H), 2.35 (dd, 1H, J = 14.5, 7.1 Hz), 2.50−2.59 (m, 1H), 2.65 (dd, 1H, J = 14.5, 6.7 Hz), 4.55 (s, 1H), 4.69 (s, 1H), 10.8 (br s, 1H). ^{13}C δ 25.08, 28.42, 34.05, 35.58, 37.77, 39.54, 105.44, 151.21, 179.23. Anal. Calcd for $C_9H_{14}O_2$: C, 70.10; H, 9.15. Found: C, 70.07; H, 9.03.

1-[2-(2-Methylenecyclohexyl)acetoxy]-2(1*H*)-pyridinethione (16). Carboxylic acid **15** (0.103 g, 0.67 mmol), 2-mercaptopyridine *N*-oxide (0.085 g, 0.67 mmol), and DMAP (7.80 mg, 0.06 mmol) were dissolved in CH_2Cl_2 (10 mL). The reaction flask was covered with foil to protect it from light, and DCC (0.151 g, 0.73 mmol) in CH_2Cl_2 (5 mL) was added dropwise over 20 min. The bright yellow reaction mixture was allowed to stir for 16 h at ambient temperature. The dicyclohexylurea was filtered off, and the yellow filtrate was concentrated. PC (35% EtOAc in hexanes) provided the pure PTOC ester **16** as a viscous yellow oil (0.144 g, 82%). FTIR (KBr) 1807, 1607, 1526, 1447, 1422, 1133, 1056. ^1H NMR δ 1.23−1.79 (m, 5H), 1.92−2.01 (m, 1H), 2.06−2.14 (m, 1H), 2.29−2.37 (m, 1H), 2.70−2.76 (m, 1H), 2.75 (dd, 1H, J = 18.2, 7.3 Hz), 3.01 (dd, 1H, J = 18.2, 9.5 Hz), 4.64 (s, 1H), 4.76 (s, 1H), 6.62 (td, 1H, J = 6.9, 1.7 Hz), 7.20 (ddd, 1H, J = 8.8, 6.9, 1.4 Hz), 7.53 (dd, 1H, J = 6.9, 1.4 Hz), 7.69 (dd, 1H, J = 8.8, 1.7 Hz). ^{13}C NMR δ 24.75, 28.28, 34.00, 35.10, 35.30, 39.38, 105.92, 112.52, 133.48, 137.39, 137.68, 150.73, 168.24, 175.92.

Kinetic Experiments. A stock solution of the PTOC ester (0.02 M in THF) containing a hydrocarbon standard was prepared. A 2.0 mL aliquot was taken and placed in a N_2-flushed test tube and capped with a rubber septum. With stirring, the solution was equilibrated to the desired temperature, and the hydride agent was added via syringe. A 200 W tungsten bulb was placed within 0.5 m of the tube, and the reaction was stirred until no PTOC ester was present per TLC (TLC taken ∼60 s after the reaction was initiated). When

tributylstannane is used as the hydride source, the completion of the reaction may be judged by the loss of the yellow color of the solution (also confirmed by TLC). Isothermal experiments were conducted simultaneously. The reactions were analyzed immediately afterward by capillary gas chromatography.

Acknowledgment. This work was supported by NSF. We thank Dr. Babak Borhan for his help at the initial stages of the modeling work.

Supporting Information Available: ^{1}H NMR, ^{13}C NMR, and FTIR spectra for compound **12**, Cartesian coordinates for HF/6-31G* optimized structures, atomic spin densities, total electronic energies, reaction parameters, and relative barriers (12 pages). This material is contained in libraries on microfiche, immediately follows this article in the microfilm version of the journal, and can be ordered from the ACS; see any current masthead page for ordering information.

JO981708N